Eksplorium *p*-ISSN 0854-1418
Volume 43 No. 2, November 2022: 89–102 *e*-ISSN 2503-426X

Geological Structure Control on the Formation of Metal Mineralization at Quartz Veins in Jendi Village, Wonogiri Regency, Central Java

Asmoro Widagdo[1]*, I Gde Sukadana[2], Frederikus Dian Indrastomo[2]
[1]Geological Engineering, University of Jenderal Sudirman (UNSOED)
Mayjen Sungkono St., Km. 5, Blater, Purbalingga, Central Java, 53371, Indonesia
[2]Center for Nuclear Fuel Cycle and Radioactive Waste Technology-BRIN
Building 720, KST B.J. Habibie, Serpong, South Tangerang, Banten, 15314, Indonesia
*E-mail: asmoro.widagdo@unsoed.ac.id

Article received: 19 May 2022, revised: 29 November, accepted: 30 November 2022
DOI: 10.17146/eksplorium.2022.43.2.6623

ABSTRACT

Quartz veins in the Jendi area and its surroundings are formed by geological structures with distributions and patterns that need to be known. This study uses data on striation, quartz vein orientation, and metal content in quartz veins. The use of this data aims to determine the relationship between the vein direction pattern and its metal mineral content with the main structure that forms it. The results of this study can be useful in determining the structural model and distribution of veins in the study area. The research method was carried out through a series of field and laboratory work. Fieldwork includes measuring striation data, measuring the orientation of quartz veins, and taking quartz vein samples. Studio work includes stereographic analysis of striation data, rosette diagram analysis of vein measurement data, and analysis of metallic element content of quartz veins. The quartz vein mineralization zone in the study area is controlled by a right slip fault with a northwest-southeast trend that forms a transtension zone with a north-south trend. The north-south trending veins are generally thick, long/continuous, and have a high metal content.

Keywords: veins, streaks, metal, faults, mineralization

INTRODUCTION

The world's demand for metallic minerals has increased in the last decade, most importantly gold [1]. The presence of gold deposits in the world is always related to magmatic/volcanic activity with host rock in the form of volcanic rocks [2]-[5] and influenced by specific geological structures [6]-[12].

Several studies on geological/tectonic structure [13] and mineralization [14]-[17] have been conducted in the study area previously. However, these studies have not provided an answer to the relationship between the fault structure that works based on the data of scratches with the veins that develop in the study area. This study seeks to answer the main type of structure acting in the Jendi area and its surroundings based on the strike-slip data on the fault plane and its relation to the pattern of metallic mineral veins developed. In addition, the research area and its surroundings are considered interesting as a research area because of the development of traditional mining owned by local residents, so it is necessary to study the geological conditions of the existing mineral structures and veins.

The occurrence of magmatic-hydrothermal fluid flow is coupled with the products of rock deformation (brecciation or faulting). Therefore, mineralization in the form of veins (mineral-filled tensile brecciation) provides useful information on

the nature and evolution of the fault system in which mineralization in veins is localized [18]. This study will provide knowledge on how the strike-slip fault system [13],[16],[19] in the study area evolved and through this evolution, provide insight into the structural controls on the formation of ore-bearing epithermal quartz veins [16],[19],[20],[21] as well as knowing where the optimum conditions for vein formation occur.

The research area is located in Jendi Village, Selogiri Subdistrict, Wonogiri Regency, Central Java Province (Figure 1). The area is about 50 km east of Yogyakarta or about 30 km south of Surakarta. Geologically, the study area is included in the South Mountains of eastern Java on the north side, bordering the Solo Depression physiography.

Figure 1. Location of the study area on the northern side of the Southern Mountains of Central Java Province.

METHODOLOGY

The research was conducted in a series of field and laboratory works. The fieldwork includes the measurement of slickenside data on the fault plane (Figures 2a and 2b), measurement of the position of quartz veins, and collection of quartz vein samples. The strike and dip of the fault plane, the angle of strike pitch (degrees), the direction of strike opening, and the type of fault movement were recorded. The strike and dip of the fault plane are measured using a geological compass, while the pitch angle is measured using a degree protractor. The type of fault movement (right shear, left shear, up or down) was determined in the field by looking at step structures and other structures on the fault plane. Quartz veins were measured for their strike and dip positions (Figure 2:f). Studio work included stereographic analysis of the streak data (Figures 2c, 2d, and 2e), flower diagram analysis of the vein measurement data, and analysis of the metal content of the veins. The line-scratch analysis will generate relationships between the main forces and the structures they produce (Figures 2c, 2d, and 2e). While the flower diagram analysis of the quartz veins will produce a general direction in the direction of the strongest main force (Figure 2f).

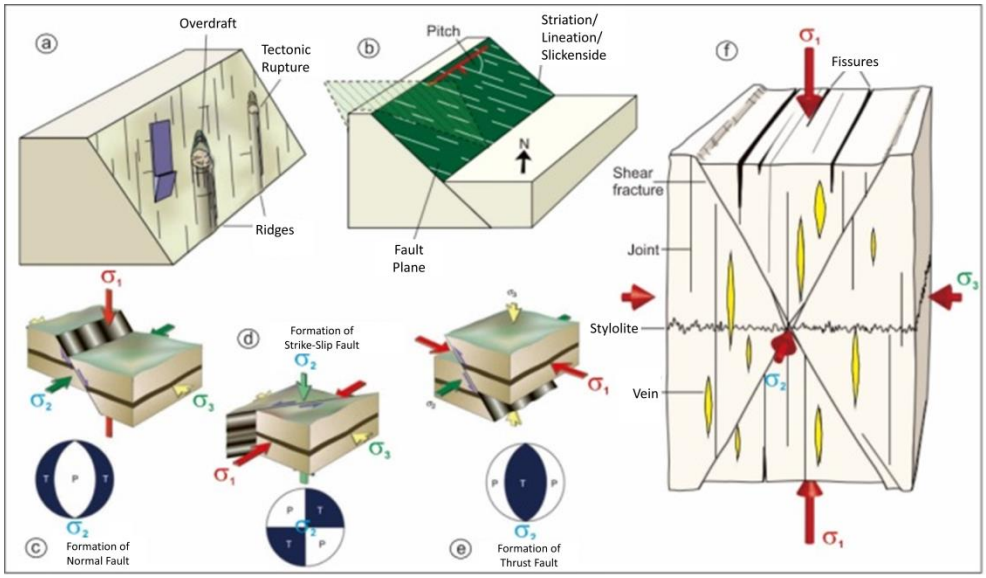

Figure 2. Basic field identification and analysis of the relationship between the main force, fault type, and general direction of veins formed in the field [22].

RESULTS

Faults Measurement

A total of nine (9) slickensides were measured on igneous andesite and microdiorite (Table 1). The observed slickenside indicates right horizontal and normal fault types. The field appearances of these slickensides are shown in Figures 3a and 3b. The slickenside with pitch angles of almost flat or less than 45^o indicates horizontal movement (Figure 3a). The observation of the step or staircase structure on the fault plane indicates a right-dipping or dextral fault type. Fault planes with slickenside with an almost vertical pitch angle (Figure 3b) or greater than 45° indicate normal or strike-slip faulting.

In the Sukamerta area, west of the study area (Figure 4), a fault plane with a strike/dip position of N 313^o E/63^o NE is observed. The slickenside on this fault plane has a pitch angle of 23^o and opens to the southeast (SE). Observation of the step/stair structure on this fault plane indicates a right horizontal or dextral movement (Table 1).

In the Nglenggong area, in the central part of the study area (Figure 4), a fault plane with a strike/dip position of N 140^o E/64^o SW is found. The slickenside on this fault plane has a pitch angle of 5^o and is open to the northwest (NW). Observation of the step/stair structure on this fault plane indicates a right horizontal or dextral movement (Table 1).

Table 1. Field measurement results and analysis of main fault forces.

No	Location	Strike/Dip	Pitch	Direction	σ_1	σ_2	σ_3
1	Sukamerta	N 313^o E/63^o NE	23^o SE	dextral	35^o/N 171^o E	55^o/N 1^o E	05^o/N 264^o E
2	Nglenggong	N 140^o E/64^o SW	5^o NW	dextral	21^o/N 1^o E	64^o/N 220^o E	15^o/N 97^o E
3	Bulu	N 135^o E/77^o SW	9^o SE	dextral	08^o/N 012^o E	76^o/N 247^o E	11^o/N 103^o E
4	Bulu	N 159^o E/78^o W	4^o N	dextral			
5	Tumbu	N 339^o E/83^o NE	25^o NW	dextral			
6	Tumbu	N 349^o E/86^o NE	19^o S	dextral	03^o/N 203^o E	86^o/N 72^o E	03^o/N 293^o E
7	Tumbu	N 320^o E/89^o N	5^o SE	dextral			
8	Melik	N 315^o E/55^o NE	20^o SE	dextral	37^o/N 169^o E	50^o/N 13^o E	12^o/N 268^o E
9	Tumbu	N 14^o E/86^o E	68^o S	normal	45^o/N 262^o E	22^o/N 16^o E	37^o/N 123^o E
10	Janggleng	N 189^o E/67^o W	75^o S	normal	64^o/N 124^o E	14^o/N 3^o E	21^o/N 268^o E

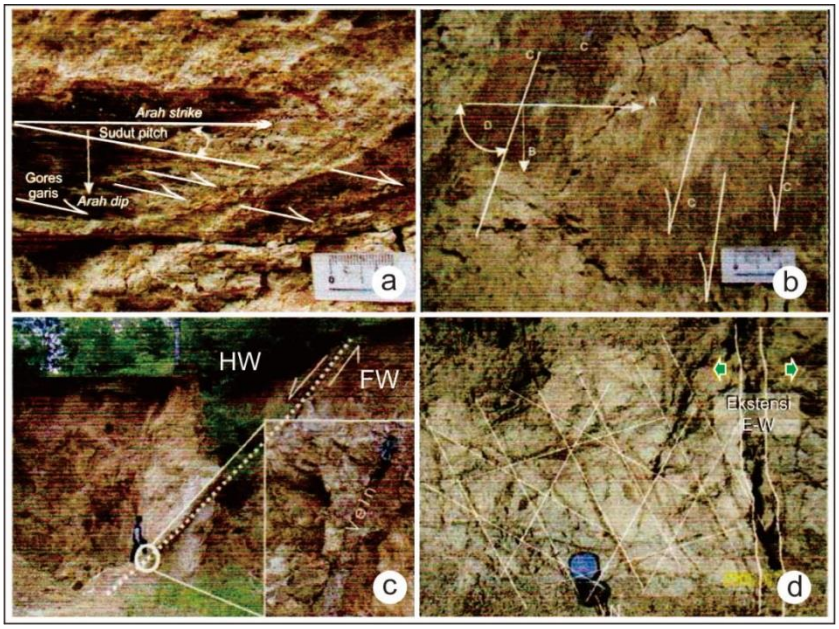

Figure 3. Geological structure and general direction of the veins in the study area. a). Right horizontal fault lines, b). Normal fault slickenside, c). Normal fault with hanging wall (HW) moving relatively down against footwall (FW), d). North-south trending veins and intensive bridging in the vicinity.

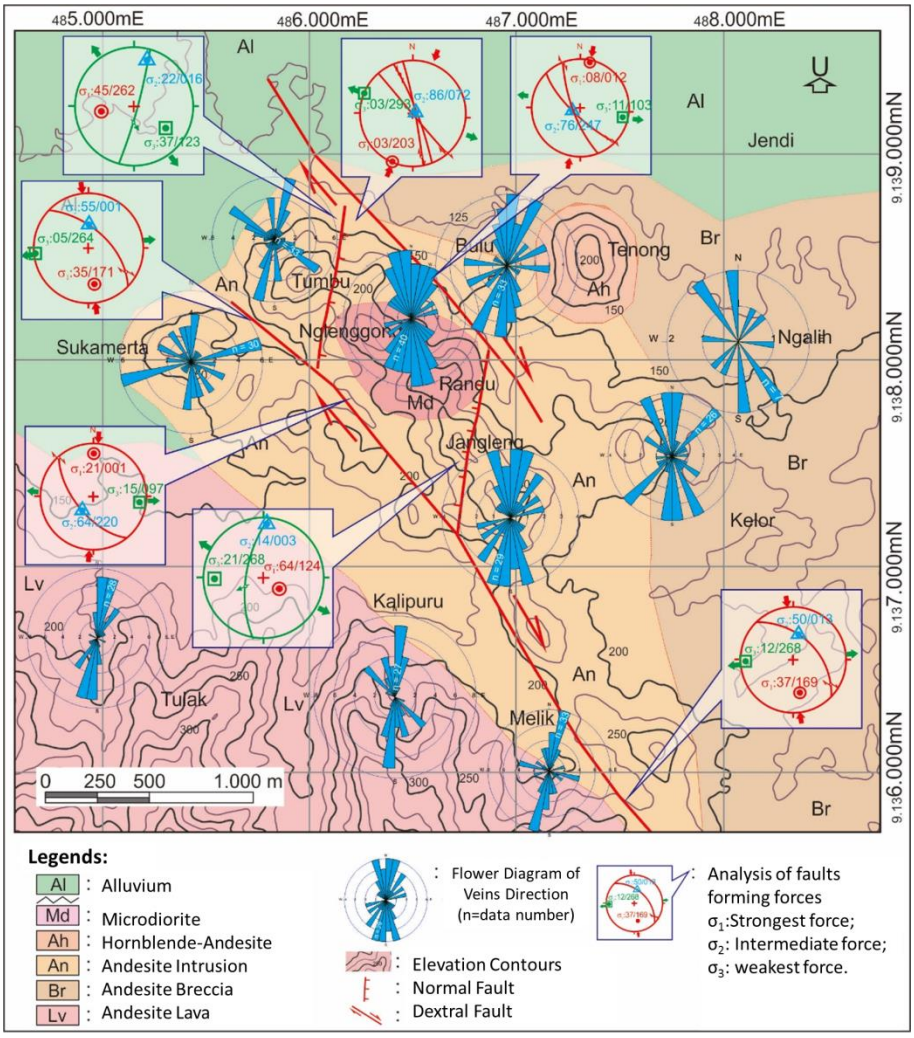

Figure 4. Geological structure and general direction of the veins in the study area.

In the Bulu area, in the central part of the study area (Figure 4), a fault plane with a strike/dip position of N 135^o E/77^o SW is observed. The striations on this fault plane have a pitch angle of 9^o and open to the southeast (SE). Observation of the step structure on this fault plane indicates a right horizontal or dextral movement (Table 1). Another fault plane at the same location in the Bulu area is found with a strike/dip position of N 159^o E/78^o W. The striations on this fault plane have a pitch angle of 4^o and open to the north. The step structure on this fault plane indicates a right horizontal or dextral movement (Table 1).

In the Tumbu area, the northwest side of the study area (Figure 4), fault planes with strike/dip positions of N 339^o E/83^o NE, N 349^o E/86^o NE, and N 320^o E/89^o N are observed. The slickensides of these three fault planes have pitch angles of 25^o opening to the northwest (NW), 19^o opening to the south (S), and 5^o opening to the southeast (SE). Observation of the step structure on these three fault planes indicates a right horizontal or dextral movement (Table 1).

In the Melik area, in the southeastern part of the study area (Figure 4), a fault plane with a strike/dip of N 315^o E/55^o NE is observed. The striations on this fault plane have a pitch angle of 20° and open to the southeast (SE). Observation of the step structure on this fault plane shows a right horizontal or dextral movement (Table 1).

In the Gunung Tumbu area, in the northwestern part of the study area (Figure 4), a fault plane with a strike/dip position of N 14^o E/86^o E is observed. The striations on this fault plane have a pitch angle of 68^o and open to the south (S). Observation of the step structure on this fault plane shows downward movement or normal fault (Table 1).

In the Janggleng area, in the central part of the study area (Figure 5), a fault plane with a strike/dip of N 189^o E/67^o W is observed. The striations on this fault plane have a pitch angle of 75^o and open to the south (S). The step structure on this fault plane shows downward movement or is a normal fault plane (Table 1).

Faults Analysis

Based on the strike-slip data collected in the field, two horizontal faults and two normal faults can be mapped in the study area (Figure 4). The two horizontal faults are the horizontal fault on the north side and the horizontal fault on the south side. Meanwhile, the two normal faults are the west-side and east-side normal faults.

Five (5) northern horizontal fault data were collected from the northern Tumbu and Bulu areas. This northern horizontal fault is formed by the strongest main force (σ_1) with a trend of N 12^o E (Bulu) and N 203^o E (Tumbu) or north-south (N-S) direction. The strongest compressional force has a relatively horizontal plunge of 8^o and 3^o. This fault is formed by the weakest main force (σ_3), which is also horizontal (11^o/N 103^o E and 3^o/N 293^o E), as presented in Table 1 and Figure 4. Based on the results of striations data analysis, the strongest main force (σ_1) formed is relatively horizontal (8^o and 3^o) or formed with the direction of the strongest main force relatively horizontal. The weakest main force (σ_3) has a plunge value that is also small/horizontal (11^o and 3^o) with a west-east direction. The combination of these forces will form a horizontal fault/shear fault [22] (Figure 2d). With the main compressional force in the north-south direction, a dextral fault in the northwest-southeast (NW-SE) direction will be formed.

The southern horizontal fault data was collected from Sukamerta, Nglenggong, and Melik. This southern horizontal fault is formed by the strongest main force (σ_1) with a trend of N 171^o E (in the Sukamerta area), N 1^o E (Nglenggong), and N 169^o E (Melik) or relatively north-south (N-S) direction. This strongest compressional force has a relatively horizontal plunge of 35^o, 21^o, and 37^o. This fault is formed by the weakest main force (σ_3), which is also horizontal (5^o/N 264^o E; 15^o/N 97^o E and 12^o/N 268^o E), as presented in Table 1 and Figure 4. Based on the results of scratch-line data analysis, where the strongest main force (σ_1) is relatively horizontal or horizontal. The weakest main force (σ_3) has a plunge value that is also small or horizontal with a west-east direction. The combination of these forces will form a horizontal fault/shear fault [22] (Figure 2d). With the main compressional force in the north-south direction, a dextral fault in the northwest-southeast (NW-SE) direction will be formed.

The western normal fault is formed by combining main forces, as shown in Figure 4. In this structural analysis result, σ_3 is at the edge of the great circle/horizontal, and σ_1 is relatively in the center or vertical. With the strongest main force vertical (45^o/N 262^o E) and the weakest main force horizontal (37^o/N 123^o E), a normal fault or strain tectonic area is formed. The strongest vertical main compression force (σ_1) and the weakest horizontal main force (σ_3) that have been acting on this fault line create a normal fault with dipping to the east.

The normal fault in the east is formed by a combination of main forces, as shown in Figure 4. In the analysis of this structure, σ_3 is at the edge of the great circle or horizontal, and σ_1 is relatively in the center or vertical. With the strongest main force vertical (64^o/N 124^o E) and the weakest main force horizontal (21^o/N 268^o E), a normal fault is formed or is a strain tectonic area. The strongest vertical main compression force (σ_1) and the weakest horizontal main force (σ_3) that have been acting on this fault line create a normal fault with dipping to the west.

Veins Measurement

Veins are open fractures filled with minerals, mainly quartz and metallic minerals (Figure 3c and d). The measured veins in this study are those with a thickness at least 1 cm. The veins measurement in the study area was done by dividing the study area into 10 sections (Table 2) based on their position in the existing geological structure constellation. This division is limited by contrasting geological or morphological structures in the study area. A flower diagram of the veins measurement results in 10 sections of the study area is illustrated in Figure 5.

Based on the results of veins measurements, the data collected is abundant (more than 30 data), including in Gunung Tumbu (35 veins), Randu (40 veins) and Bulu (35 veins), and Melik (33 veins). Areas with a moderate number of veins (20 to 30 data) include Sukamerta (30 veins), Janggleng (30 veins), Kelor (26 veins), Tulak (28 veins), and Kalipuru (27 veins). The Ngalih area on the eastern side of the study area has a sparse number of veins, with only 8 measurements.

The veins in the Gunung Tumbu area (northwestern part of the study area) are observed from 1 to 15 cm thick. Based on the flower diagram analysis (Figure 4), the general direction of these quartz veins is N 10^o–20^o E and N 300^o–310^o E or relatively north-south (N-S) and northwest-southeast (NW-SE). Based on field observations, the thicker the vein, the longer the dip in this area.

Veins in the Randu area (the central part of the study area) are found with a thickness of 1 to 10 cm. Based on the flower diagram analysis (Figure 4), the general direction of these quartz veins is N 340°–360° E or relatively north-south (N-S). Based on field observations, the veins in this area are found with high density.

The veins in the Bulu area (northern part of the study area) are found to be 1 to 10 cm thick. Based on the flower diagram analysis (Figure 4), the general direction of these quartz veins is N 0°–10° E and N 20°–30° E or relatively north-south (N-S) and north northeast-south southwest (NNE-SSW). The thick veins in this area are generally of high continuity.

Table 2. Field measurement results of quartz vein direction.

No	Location									
	Gunung Tumbu	Randu	Bulu	Suka-merta	Jang-gleng	Kelor	Tulak	Kali-Puru	Melik	Ngalih
1	300°/65°	190°/88°	28°/88°	250°/65°	185°/56°	120°/88°	11°/65°	317°/78°	191°/61°	20°/75°
2	315°/56°	153°/73°	50°/87°	70°/85°	30°/50°	1°/64°	15°/63°	342°/84°	189°/67°	68°/43°
3	100°/84°	120°/76°	60°/82°	235°/47°	336°/46°	225°/68°	20°/80°	185°/45°	180°/70°	326°/61°
4	280°/45°	122°/80°	300°/60°	250°/60°	13°/82°	203°/80°	21°/88°	1°/74°	185°/60°	170°/85°
5	195°/63°	320°/58°	294°/77°	325°/67°	10°/75°	150°/66°	10°/84°	185°/63°	298°/82°	270°/85°
6	220°/78°	170°/75°	344°/74°	41°/73°	30°/86°	180°/67°	55°/86°	335°/87°	195°/80°	355°/82°
7	192°/89°	315°/85°	20°/86°	1°/63°	34°/67°	354°/66°	293°/88°	18°/70°	160°/86°	40°/88°
8	314°/40°	170°/88°	72°/39°	317°/84°	250°/51°	185°/73°	350°/89°	15°/88°	170°/64°	141°/63°
9	294°/66°	70°/78°	220°/86°	30°/75°	236°/74°	145°/88°	210°/63°	140°/88°	175°/60°	
10	354°/84°	185°/80°	180°/64°	110°/80°	238°/51°	179°/81°	215°/60°	130°/80°	30°/88°	
11	53°/88°	30°/70°	270°/14°	295°/73°	220°/78°	4°/89°	30°/65°	181°/80°	355°/66°	
12	302°/75°	205°/83°	351°/80°	359°/66°	70°/43°	315°/73°	40°/70°	130°/82°	180°/55°	
13	356°/76°	175°/63°	188°/78°	9°/70°	159°/81°	48°/83°	248°/80°	130°/78°	205°/85°	
14	350°/71°	345°/75°	60°/87°	3°/68°	70°/52°	45°/56°	185°/87°	295°/88°	10°/87°	
15	25°/71°	320°/65°	24°/65°	250°/84°	209°/60°	242°/79°	10°/88°	1°/85°	348°/72°	
16	290°/75°	230°/75°	5°/88°	346°/75°	345°/87°	45°/86°	3°/87°	6°/75°	345°/80°	
17	10°/74°	230°/80°	174°/80°	72°/80°	140°/67°	170°/75°	2°/85°	175°/56°	280°/88°	
18	23°/86°	210°/80°	172°/77°	344°/75°	304°/66°	155°/84°	15°/84°	195°/80°	200°/88°	
19	303°/59°	210°/75°	20°/55°	350°/70°	135°/83°	231°/71°	9°/70°	345°/60°	120°/85°	
20	300°/88°	350°/80°	165°/84°	205°/75°	190°/65°	266°/87°	8°/72°	170°/56°	10°/79°	
21	168°/35°	2°/89°	65°/70°	320°/72°	341°/57°	13°/72°	170°/75°	335/85	195°/88°	
22	167°/60°	200°/84°	185°/84°	90°/64°	195°/89°	350°/84°	1°/75°	185°/70°	20°/81°	
23	265°/74°	330°/75°	98°/87°	300°/70°	351°/66°	330°/60°	358°/85°	340°/73°	74°/85°	
24	275°/74°	150°/89°	11°/79°	78°/50°	5°/65°	150°/85°	5°/83°	19°/80°	255°/80°	
25	5°/70°	250°/65°	20°/70°	350°/70°	350°/80°	122°/85°	167°/58°	354°/60°	285°/88°	
26	10°/80°	315°/89°	15°/88°	163°/65°	344°/70°	117°/78°	30°/67°	160°/74°	310°/85°	
27	11°/80°	15°/85°	185°/75°	325°/50°	177°/60°		11°/65°	200°/62°	10°/72°	
28	15°/80°	20°/86°	350°/78°	8°/84°	340°/65°		15°/63°		305°/85°	
29	320°/69°	28°/59°	160°/85°	270°/83°	181°/85°				280°/80°	
30	290°/80°	225°/78°	158°/60°	290°/72°	185°/86°				185°/70°	
31	155°/60°	195°/80°	190°/72°						280°/70°	
32	200°/80°	348°/89°	95°/70°						190°/80°	
33	35°/75°	349°/85°	40°/80°						190°/85°	
34	300°/75°	339°/83°	155°/80°							
35	350°/75°	17°/73°	275°/80°							
36		165°/72°								
37		183°/89°								
38		350°/69°								
39		181°/76°								
40		349°/86°								

The veins in the Melik area (southern part of the study area) have a thickness range from 1 to 6 cm. Based on the flower diagram analysis (Figure 4), the general direction of the quartz veins is N 10°–20° E or relatively north-

south (N-S). The veins in the Melik area are found to be very dense and continuous.

Veins in the Sukamerta area (western part of the study area) are found with a thickness of 1 to 5 cm. Based on the flower diagram analysis (Figure 4), the general direction of the quartz veins is N 250^o–260^o E and N 0^o – 10^o E or relatively southwest-northeast (WSW-ENE) and north-south (N-S). The veins in this area are generally of low dip or not long. The veins in the Janggleng area (the central part of the study area) are found with a thickness of 1 to 10 cm. Based on the flower diagram analysis (Figure 4), the general direction of the quartz veins is N 340^o–350^o E and N 0^o–20^o E or relatively north-south (N-S). The thick veins in this area generally have high dips. Veins in the Kelor area (eastern part of the study area) are found with a thickness of 1 to 6 cm. Based on the flower diagram analysis (Figure 4), the general direction of these quartz veins is N 350^o–360^o E and N 40^o–50^o E or relatively north-south (N-S) and northeast-southwest (NE-SW). The population of veins in this area is very sparse and short. The veins in the Tulak area (southwestern part of the study area) are found with a thickness of 1 to 5 cm. Based on the flower diagram analysis (Figure 4), the general direction of these quartz veins is N 0^o–10^o E or relatively north-south (N-S). The veins in this area are very rare and short. The veins in the Kalipuru area (southern part of the study area) are found with a thickness of 1 to 5 cm. Based on the flower diagram analysis (Figure 4), the general direction of these quartz veins is N 0^o–10^o E or relatively north-south (N-S). The spacing of the veins in the Kalipuru area is generally tenuous, with long dimensions that are not continuous. The veins in the Ngalih area (eastern part of the study area) are found with a thickness of 1 to 3 cm. Based on the flower diagram analysis (Figure 4), the general direction of these quartz veins is N 350^o–360^o E or relatively north-south (N-S) and N 320^o–330^o E or relatively northwest-southeast (NW-SE). The quartz veins in this area are very rare and short.

Metal Contents

To determine the content of metal elements in quartz veins in the study area, laboratory analysis of five (5) vein samples from different locations was carried out. The analysis was conducted to determine the content of metallic elements of gold (Au), silver (Ag), copper (Cu), lead (Pb), and zinc (Zn). The results of the elemental metal content analysis in ppm (parts per million) are presented in Table 3.

Table 3. Results of metal content analysis on quartz veins.

No	Location	Vein Orientation	Metal Content (ppm)				
			Au	Ag	Cu	Pb	Zn
1	Tumbu	NW-SE	--	--	100	63	32
2	Randu	N-S	204	411	57,797	2,311	22,356
3	Bulu	NE-SW	--	350	8,200	--	20,300
4	Janggleng	N-S	5.2	29	330	1,130	170
5	Sukamerta	E-W	9.8	64	100	1,010	690
6	Melik	N-S	2.4	25	330	1,330	2,480

The analysis of the northwest-southeast (NW-SE) trending quartz vein from Mount Tumbu in the north of the study area shows the absence of gold and silver. Only copper, lead, and zinc were found in this vein (Table 3). The vein is directed N 155^o E/60^o SW with a thickness of 1 cm. The direction of the

vein is in line with the direction of the main horizontal fault in the study area.

The vein from the Randu area was taken from the N 185^o E/80^o W vein with a thickness of 2 cm. This north-south trending vein contains metallic elements of gold, silver, copper, lead, and zinc (Table 3).

The northeast-southwest trending vein was taken from the Bulu area in the northern part of the study area. Samples were taken from the N 50^o E/87^o SE oriented vein with a vein thickness of 3 cm. No gold was found in this vein. Silver, copper, lead, and zinc were found in this northeast-southwest (NE-SW) trending vein.

The vein sample from the Janggleng area was taken at the N 185^o E/86^o W aligned vein with a thickness of 4 cm. This north-south (N-S) aligned vein contains metallic elements of gold, silver, copper, lead, and zinc.

The vein content from the Sukamerta area was analyzed on a relatively west-east (E-W) oriented vein. The position of this vein is N 295^o E/73^o N with a thickness of 1 cm. This vein contains metallic elements of gold, silver, copper, lead and zinc.

The vein from the Melik area is N 195^o E/88^o W (north-south vein) with a thickness of 2 cm. This north-south (N-S) trending vein contains metallic elements of gold, silver, copper, lead, and zinc (Table 3).

DISCUSSION

Based on rock mapping in the field (Figure 4), quartz veins in the study area are mainly formed in andesite and microdiorite intrusive rocks. These rocks are faulted by a northwest-southeast (NW-SE) trending right horizontal fault. This right horizontal fault plays an important role in volcanism and magmatism [8],[9] and mineralization [23], [24] in the study area. The study area is part of the central facies of the Gajah Mungkur ancient volcano [2],[25]. The emergence of the Gajah Mungkur ancient volcano was strongly influenced by tectonics [26] as the driver of the faults in the study area.

The presence of geological structures is linearly proportional to the intensity of alteration and mineralization [11]. Mineralization in the study area only occurs in the extension zone and around the main fault. Far to the east and southwest, quartz veins are rarely found. The right horizontal fault in the study area was very active during its period, giving rise to various rocks from a deeper formation environment. These rocks are extrusive rocks (andesite lava on the surface), explosive rocks (breccia on the surface), and shallow intrusive rocks (andesite) to deep intrusive rocks (microdiorite). In the final phase, this main fault caused all these rocks to be deformed to form shear fractures and extension fractures. Deeper magmatism produces hydrothermal solutions that move upwards and fill the fractures. It is widely accepted and proven in many locations that faults control the settlement of magma and hydrothermal fluids [8]. These fractures filled with metallic mineral deposits are then known as quartz veins.

Multi-stage deformation structures have also been found in other gold-mineralized areas [7]. The presence of veins intersected by younger veins in the study area supports the existence of multiple mineralizations. These quartz veins follow the orientation of the extension joints, which were previously formed by geological structures due to the forces acting at the time. This condition is in line with research that mentions the existence of tectono-magmatic that controls metallic mineral deposits [9].

The orientations of the main tectonic forces are significant in determining the

evolution of geological structures in an area [27]. The north-south (N-S) oriented tectonic force (σ_1) acting on Java Island is the main control of vein orientation in the study area. The relationship of the dextral fault to the formation of normal faults and extension zones is shown in Figure 6. This model explains the structural constellation in the study area. The dextral faults in the north and south parts form an en-echelon right-stepping pattern where there is an overlap between the two horizontal faults [28]. This overlap zone then forms a normal fault in the central part of the study area. The normal fault to the west (Nglenggong area) has an eastward dip and a westward dip to the east (Janggleng area). The extension zone at the intersection of these two right horizontal faults is the main mineralized area in the study area (the area around Bukit Randu). Quartz veins with high thickness and density are found in this extension zone. The north-south (N-S) trending veins of this extension zone also show a high content of metallic elements, especially gold.

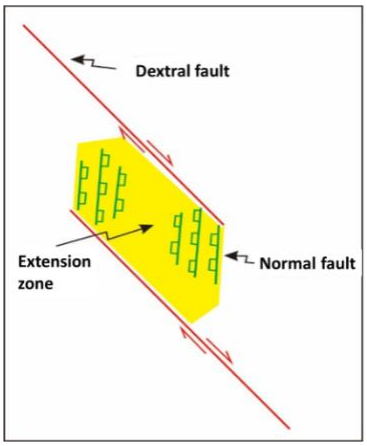

Figure 6. En-echelon right-stepping horizontal fault model that forms an extension zone [28].

During convergent orogenic events or plate collisions, tectonic stresses affect rocks over a wide area. Joints are syntectonic because they are parallel to the direction σ_1 associated with the development of tectonic structures. In addition, faults locally contain mineral fillings formed at fluid temperatures and pressures at depths of several kilometers from the surface [23]. The north-south (N-S) trending veins in the study area are aligned with the direction of regional compression (σ_1) originating from the south or the direction of plate subduction [29],[30]. This compression forms an east-west (E-W) pull which is the direction of extension or vein opening (Figure 8a).

The north-south (N-S) trending veins formed from the main north-south (N-S) trending compressional forces in the study area have a wide range of directions. The distribution of this vein direction is in the range of N 325^o E and N 35^o E, as shown in the flower diagram (Figure 4). As a result of the north-south oriented force σ_1, an extension joint will form as a space for vein formation in the 75^o E range (Figure 7) [31]. Rose diagram analysis of quartz veins in the study area shows that the general direction of the veins is still within this range.

Quartz veins oriented approximately northeast-southwest (NE-SW), northwest-southeast (NW-SE), and west-east (E-W) may be present in association with the shear joints range (Figure 7) as a result of compression from the same north-south direction [31]. Shear joints resulting from regional compression (σ_1) in a north-south direction form right horizontal faults in the north and south of the study area with a range of 135° (Figure 7). Initially, these joints are dense (Figure 8b), making it impossible for the flow and deposition of vein-forming hydrothermal solutions. However, these shear joints may open when reactivated by younger tectonics [13]. These fractures will become hybrid fractures, where they initially fracture and then open, as shown in Figure 8c [28].

p-ISSN 0854-1418
e-ISSN 2503-426X

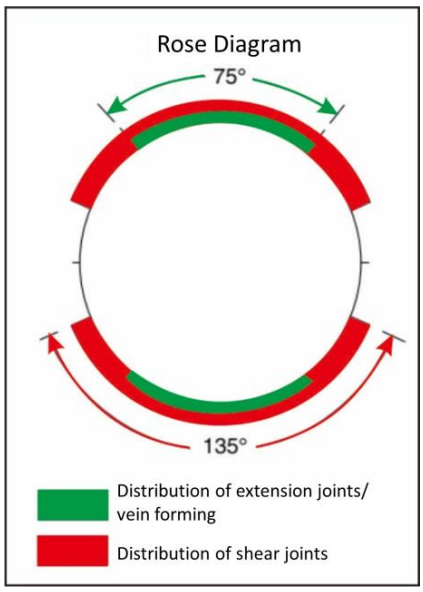

Figure 7. Directional distribution of extension fracture-filling quartz veins due to north-south force [31].

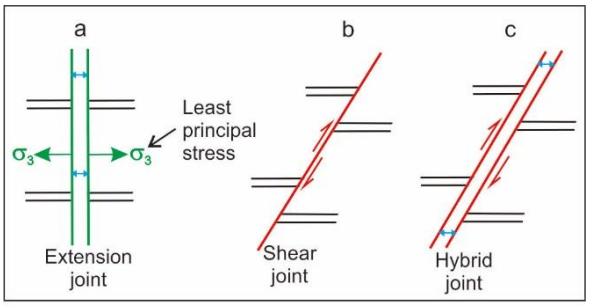

Figure 8. Types of joints [28].

The extension veins in the study area are generally of a high thickness (1-20 cm), where the thicker the vein, the longer it will generally be. The veins are also vertically continuous with a high degree of continuity. This allows hydrothermal solutions carrying metallic minerals to pass easily from the high-pressure zone at depth towards the surface. Areas that far from the extension zone, like Kelor and Ngalih (east of the study area), have rare vein distributions. The veins in these areas are also generally short and poorly filled with metallic minerals. This is also the case in the Tulak area located in the southwest of the study area, which is far from the main dextral fault extension zone.

CONCLUSION

The northwest-southeast trending en-echelon right-stepping dextral fault in the study area forms an extension zone that becomes the main quartz vein mineralization zone. Quartz veins generally form in a north-south (N-S) direction parallel to the main regional compressional forces that form the northwest-southeast (NW-SE) dextral fault and the north-south (N-S) normal fault. The northwest-southeast, northeast-southwest, and west-east trending quartz veins are formed by hybrid fracturing as a progression of activated shear joints. The north-south (N-S) oriented veins are generally thick, long, continuous, and have high metal content. The veins in other directions are generally short and thin.

ACKNOWLEDGEMENT

For the completion of the research for this publication, the author would like to acknowledge colleagues at the Department of Geological Engineering, Universitas Jenderal Soedirman-Purwokerto (Ir. Adi Candra, ST. MT, Ir. Siswandi ST., MT, Drs. Gentur Waluyo, MSi., Huzaely Latief Sunan, ST., MT., Akhmad Kahlil Gibran, ST., MT., Januar Aziz Zaenurrohman, ST., M.Eng, Maulana Rizki Aditama, SSi., MSi, Anjar T. L, ST., M.Sc. and Dr. Ir. Eko B.. P., ST, MSi) who have been very helpful in the research process and writing of this paper.

REFERENCES

[1] Hasria, A. Idrus, and I. W. Warmada, "Endapan Emas Hidrotermal Pada Batuan Metamorf di Pegunungan Rumbia, Kabupaten Bombana, Propinsi Sulawesi Tenggara," *Prosiding Seminar Nasional Kebumian XII*, FTM-UPN 'Veteran' Yogyakarta, pp. 123-131, 2017.

[2] H. G. Hartono, S. Pambudi, M. Arifai, A. Yusliandi, and S. Agung, "Vulkanisme dan Sebaran Sumber Daya Non Hayati di Pegunungan Selatan Yogyakarta dan Wonogiri, Jawa Tengah," *Majalah Geologi Indonesia*, vol. 29, no. 1, pp. 37-47, 2014.

[3] E. D. Putranto, Suprapto, and A. Harjanto, "Studi Geologi, Alterasi dan Mineralisasi Endapan Epitermal Sulfida Tinggi, Daerah Prospek Rasik, Ayam Hitam dan Sekitarnya, Desa Lanut, Kecamatan Lodayang, Kabupaten Bolaang Mongondow Timur, Provinsi Sulawesi Utara," *Jurnal Ilmiah Geologi Pangea*, vol. 3, no. 2, pp. 45-60, 2016.

[4] A. Harjanto, Sutarto, A. Subandrio, I M. Suasta, J. Salamat, G. Hartono, P. Suputra, I. G. Basten, M. Fauzi, and Rosdiana, "Alterasi Hidrotermal Di Dumoga Barat Kabupaten Bolaang Mongondow, Sulawesi Utara," *Jurnal Eksplorium*, vol. 37 no. 1, pp. 27–40, 2016.

[5] A. S. Ubaidillah, A. Idrus, I. W. Warmada, and S. Maula, "Geokimia Pada Endapan Cu-Au Porfiri Brambang Pulau Lombok, Nusa Tenggara Barat," *Jurnal Geosapta*, vol. 5, no. 2, pp. 103-113, 2019.

[6] T. Hafizh, A. Patonah, I. Haryanto, and I. Priyowasono, "Kontrol Struktur Terhadap Mineralisasi Pada Daerah North West Di Area Tambang Batu Hijau PT Newmont Nusa Tenggara," *Padjajaran Geoscience Journal*, vol. 1, no. 3, pp. 201-206, 2017.

[7] V. Y. Fridovsky, M. V. Kudrin, and L. I. Polufuntikova, "Multi-Stage Deformation of the Khangalas Ore Cluster (Verkhoyansk-Kolyma Folded Region, Northeast Russia): Ore-Controlling Reverse Thrust Faults and Post-Mineral Strike-Slip Faults", *Journal Minerals*, vol. 8, no. 270, pp. 2-18, 2018.

[8] Y. Song, C. Yang, S. Wei, H. Yang, X. Fang, and H. Lu, "Tectonic Control, Reconstruction and Preservation of the Tiegelongnan Porphyry and Epithermal Overprinting Cu (Au) Deposit, Central Tibet, China," *Journal Minerals*, vol. 8, no. 398, pp. 1-17, 2018.

[9] J. Tuduri, A. Chauvet, L. Barbanson, J. L. Bourdier, M. Labriki, A. Ennaciri, L. Badra, M. Dubois, C. E. Leloix, S. Sizaret, and L. Maacha, "The Jbel Saghro Au (–Ag, Cu) and Ag–Hg Metallogenetic Province: Product of a Long-Lived Ediacaran Tectono-Magmatic Evolution in the Moroccan Anti-Atlas," *Journal Minerals*, vol. 8, no. 592, pp. 1-48, 2018.

[10] A. Chauvet, "Structural Control of Ore Deposits: The Role of Pre-Existing Structures on the Formation of Mineralised Vein Systems," *Journal Minerals*, vol. 9, no. 56, pp. 5-26, 2019.

[11] A. Bari, M. F. Rosana, and I. Haryanto, "Kontrol Struktur Geologi Pada Alterasi dan Mineralisasi di daerah Cibaliung Kabupaten Pandeglang, Provinsi Banten," *Buletin Sumberdaya Geologi*, vol. 15, no. 1, pp. 73-87, 2020.

[12] A. Idrus, and W. Hermansyah, "Karakteristik Mineralisasi Bijih Emas Pada Prospek Hargosari, Kecamatan Tirtomoyo, Kabupaten Wonogiri, Provinsi Jawa Tengah," *Jurnal Kurvatek*, vol. 6, no. 1, pp. 31-40, 2021.

[13] A. Widagdo, "Fase-Fase Tektonik Pembentuk Ruang Mineralisasi Emas di Daerah Selogiri, Wonogiri", *Jurnal Dinamika Rekayasa*, vol. 4, no. 1, pp. 22-29, 2008.

[14] A. Idrus, D. Y. Fatimah, and F. Hakim, "Karakteristik Alterasi dan Mineralisasi Emas Pada Sistem Epitermal Prospek Randukuning, Kecamatan Selogiri, Kabupaten Wonogiri, Jawa Tengah," *Proceeding Seminar Nasional Kebumian Ke-8*, Teknik Geologi-UGM, Yogyakarta, 2015.

[15] D. Z. Herman, "Model Fasies Gunung Api Dalam Kaitannya Dengan Ubahan Hidrotermal dan Mineralisasi di Daerah Selogiri, Kabupaten Wonogiri-Jawa Tengah," *Buletin Sumberdaya Geologi*, vol. 1, no. 1, pp. 43-53, 2006.

[16] Sutarto, A. Idrus, A. Harijoko, L. D. Setijadi, F. M. Meyer, S. Sindern, and S. Putranto, "Hydrothermal Alteration and Mineralization of the Randu Kuning Porphyry Cu-Au and Intermediate Sulphidation Epithermal Au-Base Metals Deposits in Selogiri, Central Java, Indonesia," *Journal of Applied Geology*, vol. 1, no. 1, pp. 1-18, 2016.

[17] V. B. Rahmadani, H. Bahar, S. H. Yuwanto, and L. Utamakno, "Studi Alterasi dan Mineralisasi Daerah Keloran dan Sekitarnya, Kecamatan Selogiri, Kabupaten Wonogiri, Provinsi Jawa Tengah," *Prosiding Seminar Teknologi Kebumian dan Kelautan ITATS Surabaya*, vol. 3, no. 1, pp. 482-486, 2021.

[18] B. R. Berger, "The 3D Fault and Vein Architecture of Strike-Slip Releasing and Restraining Bends: Evidence from Volcanic-Centre-Related Mineral Deposits," *Geological Society, London, Special Publications*, vol. 290, pp. 447–471, 2016.

[19] Sutarto, A. Idrus, A. Harijoko, L. D. Setijadi, F. M. Meyer, and S. Sindern, "Mineralization Style of The Randu Kuning Porphyry Cu-Au and Intermediate Sulphidation Epithermal Au-Base

Metals Deposits at Selogiri Area, Central Java Indonesia," *2nd International Conference on Earth Science, Mineral, and Energy*, 2020.

[20] A. Imai, J. Shinomiya, M. T. Soe, L. D. Setijadji, K. Watanabe, and I. W. Warmada, "Porphyry-Type Mineralization at Selogiri Area, Wonogiri Regency, Central Java, Indonesia," *Resources Geology*, vol. 57, no. 2, pp. 230-240, 2007.

[21] Sutarto, A. Idrus, S. Putranto, A. Harijoko, L. D. Setijadi, F. M. Meyer, and R. Danny, "Hydrothermal Alteration and Vein Types of The Randu Kuning Porphyry Cu-Au Deposit, At Selogiri Area, Wonogiri," *Buletin Sumber Daya Geologi*, vol. 9, no. 1, pp. 41-54, 2014.

[22] H. Fossen, *Structural Geology*, Cambridge University Press, New York, 2010.

[23] B. A. van der Pluijm and S. Marshak, *Earth Structure, an Introduction to Structural Geology and Tectonics*, 2nd edition, W. W. Norton Company, New York, 2004.

[24] B. J. Claude, T. Rigobert, E. Joachim, F. T. Periclex, and D. M. G. G. Basile, "Geological Context Mapping of Batouri GoldDistrict (East Cameroon) from Remote Sensing Imagering, GIS Processing and Field Works," *Journal of Geographic Information System*, vol. 11, pp. 766-783, 2019.

[25] O. Verdiansyah, H. G. Hartono, and O. Sugarbo, Review of The Volcanosetting Concept to Discover the Precious Metal Mineralization in Sunda Arc, Indonesia: An Approach Proposal for Mineral Exploration, 2021.

[26] O. Verdiansyah, D. Muharif, and I. G. Sukadana, "Indikasi Mineralisasi Tipe Porfiri di Daerah Sumbersari, Kompleks Pengunungan Kulon Progo, Purworejo, Indonesia," *Jurnal Eksplorium*, vol. 41, no. 2, pp. 115-128, 2020.

[27] J. Wahyudiono, C. I. Abdullah, and H. Z. Abidin, "Kontrol Sesar Terhadap Pola Sebaran Urat Kuarsa Dan Mineralisasi Emas Daerah Kutawaringin, Jawa Barat," *Jurnal Sumber Daya Geologi*, vol. 21, no. 3, pp. 163-175, 2011.

[28] K. R. Mc.Clay, *The Mapping of Geological Structures*, John Wiley and Sons, London, 2007.

[29] A. Patria, and A. N. Aulia, "Structural and Earthquake Evaluations Along Java Subduction Zone, Indonesia," *Jurnal Riset Geologi dan Pertambangan*, vol. 30, no. 1, pp. 65-79, 2020.

[30] A. Shulgin, H. Kopp, C. Meller, L. Planert, E. Lueschen, E. R. Flueh, and Y. Djajadihardja, "Structural Architecture of Oceanic Plateau Subduction Offshore Eastern Java and the Potential Implications for Geohazards,". *Geophysical Journal International*, vol. 184, pp. 12-28, 2011.

[31] B. B. S. Singhal and R. P. Gupta, *Applied Hydrogeology of Fractured Rocks*, Springer Science Business Media, 2010.